The use of computational fluid dynamics to estimate fluid residence time and flow hydrodynamics in open digesters of wastewater treatment plants: A case study

Raúl Barrio[1], Eduardo Blanco[2], Joaquín Fernández[3], Mónica Galdo[4]

Universidad de Oviedo, Departamento de Energía. Campus de Viesques, 33204 Gijón (Asturias), Spain

[1]Corresponding author. Phone: +34 985 182 284. Fax: 985 182 098. E-mail: barrioraul@uniovi.es

[2]Phone: +34 985 182 103. E-mail: eblanco@uniovi.es

[3]Phone: +34 985 188 145. E-mail: jffrancos@uniovi.es

[4]Phone: +34 985 182 247. E-mail: galdomonica@uniovi.es

Abstract

Residence time is an important parameter in mixing systems. Particularly, the performance of the processes in the digesters of wastewater treatment plants is influenced by the residence time distribution. This can be obtained experimentally by injecting inert chemicals to measure their concentration at the outlet. An alternative approach is to simulate the flow field with Computational Fluid Dynamics software. This paper explores a methodology to compute fluid residence time and investigate flow hydrodynamics in open digesters of full scale wastewater treatment plants by CFD calculations through a case study. The methodology is based on the resolution of an additional transport equation for a separate species. The concentration of this species at the outlet of the digesters is monitored and can be related with the residence time of the fluid. Furthermore, the resolution of the unsteady flow field provides a complete set of data that was used to detect stagnation or by–pass regions.

1. INTRODUCTION

Environmental safety of water effluents in wastewater treatment plants must be assured by means of a proper water management. The effectiveness of water treatment is in close relation to the time of exposure to the chemical or biological reactants presented in the reactors of the plant. In this sense, the residence time of the fluid is a parameter of significant importance in the design of reactors since it provides information about the time window that reactions could occur.

Traditionally, the residence time distribution is determined in experiments by the tracer method [1–4]. The tracer is an inert chemical that is injected at the inlet of the reactor or mixing device, either in pulse or step mode; the concentration of the tracer is measured continuously at the exit region. The temporal evolution of the tracer's concentration is used subsequently to compute the residence time distribution and also the mean residence time. However, this experimental approach is not always feasible due to the time/cost of the experiments or due to the operating constraints of the plant. Besides, it provides information only about the global behavior of the flow but without indicating any aspect of the flow hydrodynamics.

In addition to the experimental techniques, several theoretical models have been proposed in the technical literature in order to estimate the residence time distribution in a single device or set of devices [5–7]. The models range from those that ideally assume

a perfect mixing and uniform fluid properties (continuous stirred tank reactors) to those that assume absence of mixing in the direction of the flow (plug–flow reactors), or to other models designed to account for deviations from these two ideal extremes. Then again, most of the models provide only general data since the complete hydrodynamics of the flow within the reactor, which has a significant effect on its performance, is not considered.

The use of Computational Fluid Dynamics (or CFD) software is gaining in importance for the hydrodynamic simulation of either Newtonian or non–Newtonian fluid flows [8–13]. Typically, the residence time distribution at the exit of a particular device can be numerically estimated by means of Lagrangian particle tracking [14] or by the resolution of a transport equation for an additional species [15–18]. The latter approach provides also an entire description of the flow field in the device, which can be of significant interest and overrides the obvious limitations regarding the cost and the degree of detail for the case of large reactors.

This paper presents a numerical investigation on the hydrodynamics of two open biological digesters that operate in a full scale wastewater treatment plant. For this purpose, the commercial code Fluent® is applied to solve the Unsteady Reynolds–Averaged Navier–Stokes equations for a tracer fluid in a model of the digesters. The complete set of data provided by the calculations is analyzed in order to investigate the flow dynamics and also to detect stagnation and dead zones. Finally, the numerical

predictions are used to estimate the residence time distribution for the fluid at the exit section of the digesters.

2. NUMERICAL METHODOLOGY

2.1. Geometry of case study

The present work was carried out on two open digesters of a full scale wastewater treatment plant whose geometry is conditioned by space availability. The geometry of the digesters is depicted schematically in Fig.1. The wastewater flows inside digester 1 (D1) from the left. An anaerobic digestion takes place in this region while four mixers (see detail in Fig. 2) prevent decantation. Each mixer has 8 blades, an outer diameter of 2.3 m, and a nominal flow rate of 4.2 m^3 s^{-1} when running at 22 rpm. Subsequently, the flow is lead into digester 2 (D2) where two grids of 754 diffusers each (13 rows per grid) are arranged in the sense of the flow to induce streams of fresh air for the aerobic digestion. A single diffuser has an outer diameter of 0.229 m and provides an average flow of air at standard conditions of 2.78 m^3 h^{-1}.

[Figure 1 here]

The numerical model was created for each zone separately with the commercial code Gambit® from the blueprints of the plant. The vertical dimension of the model (z–axis) was limited to the depth of the fluid in the digesters, namely 3.7 m. The mesh used for the discretization of the geometry was both semi–structured and unstructured. The former was generated by means of prismatic cells with triangular base whereas tetrahedral cells were used for the latter one. This type of structure allowed for a better

5

adaptation to complex regions and also for a good vertical resolution while preventing long computational times.

[Table 1 here]

Several details on the geometry and the mesh are presented in Fig. 2. Fig. 2(a) shows the surface mesh of digester 1 with a detail of the mesh near one of the mixers. The surface mesh of the aerobic digester can be observed in Fig. 2(b) and also a detail of the mesh near the central diffusers. Table 1 shows the total number of cells in each digester and also the final size of the grid. The maximum magnitude of the equiangle skew was restricted to 0.85 to prevent an excessive cell distortion that could cause numerical dispersion in the calculations.

[Figure 2 here]

A grid dependence analysis was performed before starting the simulation routine. This analysis showed that the variations obtained in the residence time distributions (that will be presented in section 3.2) were lower than 0.5% even when doubling the density of the grid used for the final calculations.

2.2. Numerical model and calculation procedure

The numerical simulation of the two digesters was carried out with the commercial software Fluent®. This is a finite volume–based code that was used to solve the full 3D Unsteady Reynolds–Averaged Navier–Stokes equations (3D–URANS) for incompressible flow:

$$\nabla \overline{v} = 0 \tag{1}$$

$$\frac{\partial \overline{v}_i}{\partial t} + \nabla \left(\overline{v}_i \, \overline{v}_j \right) = -\frac{1}{\rho} \nabla \overline{p} + \nabla \left(v \nabla \overline{v}_i \right) - \frac{1}{\rho} \nabla \left(\rho \overline{v_i' v_j'} \right) \tag{2}$$

The temporal and spatial derivatives were discretized by means of second–order upwind schemes. The coupling between velocity and pressure was resolved by the SIMPLE algorithm. Turbulent closure was established by the RNG k–ε model together with standard wall functions based on the proposal of Launder and Spalding [19] to calculate near–wall flow, since these functions have been most widely used for industrial flows. The RNG $k - \varepsilon$ model defines two additional transport equations for the variables k and ε:

$$\frac{\partial}{\partial t}(\rho k) + \frac{\partial}{\partial x_i}(\rho k \overline{v}_i) = \frac{\partial}{\partial x_j}\left[\alpha_k \, \mu_{\text{eff}} \, \frac{\partial k}{\partial x_j} \right] + G_k + G_b - \rho \varepsilon \tag{3}$$

$$\frac{\partial}{\partial t}(\rho \varepsilon) + \frac{\partial}{\partial x_i}(\rho \varepsilon \overline{v}_i) = \frac{\partial}{\partial x_j}\left[\alpha_\varepsilon \, \mu_{\text{eff}} \, \frac{\partial \varepsilon}{\partial x_j} \right] + C_{\varepsilon 1} \frac{\varepsilon}{k}\left(G_k + C_{\varepsilon 3} G_b \right) - \rho C_{\varepsilon 2} \frac{\varepsilon^2}{k} - R_\varepsilon \tag{4}$$

where G_k and G_b represent the generation of turbulent kinetic energy due to the mean velocity gradients or to the buoyancy, α_k and α_ε are the inverse effective Prandtl numbers for k and ε, μ_{eff} is the effective viscosity, and the term R_ε accounts for the

effect of rapid strain and streamline curvature thus representing an improvement of the standard k-ε model.

The boundary conditions imposed in each digester were a constant velocity at the inlet and a constant static pressure at the outlet. A non–shear symmetry condition was established for the free surface of the fluid. Also, a no slip shear condition was imposed to the walls. The effect of gravity was not considered in the calculations.

The actual fluid of the plant is an activated mud with a concentration of solid pollutants of about 2000 ppm. According to the information provided by the company, this concentration is low enough to consider the fluid as a continuum, that is, particle interactions were not included in the simulations.

The motion of the mixers was included by defining a cylinder of fluid of 2.8 m in diameter around each of them in the computational domain. These volumes of fluid were set as moving reference frames with an angular velocity of 2.304 rad s^{-1} (i.e. 22 rpm) imposed in order to simulate the rotation of the fluid near the mixers, since the residence time distribution is influenced mainly by the transport of the tracer outside the impeller zone. The effect of the streams of air in the aerobic digester was considered by means of an additional source term included in the right–hand side of momentum equation (z–axis). This source term was calculated from the upthrust generated by the

amount of air in the volume of fluid. The amount of air was estimated from the flow in the diffusers and the typical rise velocities of air bubbles in water.

The criterion established for the convergence of the numerical calculations was to reduce the scaled residuals (sum of the quotient between the residuals and the sum of the fluxes in all mesh cells for the calculated variables) below 10^{-5} (five orders of magnitude).

The calculations were carried out in two steps. Steady–state simulations were first performed at each zone until achieving steady convergence, for which at least 3000 iterations were required. No multispecies model or particle tracking was considered during this step.

The velocity and pressure steady fields obtained were used subsequently to initialize the unsteady computations. An additional species was included in these calculations in order to be used as tracer, so that the mass fraction of the fluid at the exit boundary of the digesters can be related to the residence time, as explained in the following section. For this purpose, a non–reacting scalar transport equation for the new species was included and resolved in Fluent® by activating the multispecies model:

$$\frac{\partial(\rho m_i)}{\partial t} + \nabla(\rho \bar{v} m_i) = \nabla(\rho D_i \nabla m_i) \qquad (5)$$

being m_i the mass fraction of the new species and D_i the mass diffusivity. This approach assumes that the tracer is dispersed in the digesters only by convection and diffusion. The physical properties of the tracer fluid are the same as the original fluid (water liquid) but a different tag was assigned to it to allow identification of the species.

Two flow rates were simulated: 666 m^3 h^{-1} and 4000 m^3 h^{-1} (minimum and maximum flow rate expected for the plant). The time step size was set to 10 s for the 666 m^3 h^{-1} flow rate and to 2 s for the 4000 m^3 h^{-1} flow rate, which was consistent with the size of the cells and with the average velocities in the plant. Some preliminary tests were carried out with the purpose of estimating the number of iterations required to achieve convergence in each time step, resulting in a maximum of 20 iterations per time step. The simulations were performed until achieving a mass fraction of the tracer fluid equal to one at the exit boundary of each zone, as explained in the following section.

3. RESULTS AND DISCUSSION

3.1. Contour maps of tracer's mass fraction and velocity vectors

The numerical calculations were stored in a personal computer every 10 time steps and processed subsequently. A series of contour maps of the instantaneous mass fraction of the tracer fluid are presented in Fig. 3 (666 m^3 h^{-1} flow rate) and Fig. 4 (4000 m^3 h^{-1} flow rate) as an example of fluid renovation within the anaerobic digester. Each figure shows the spatial distribution of this mass fraction in a xz plane located at mid–span (top

image) and also in a *xy* plane located at mid–height (bottom image) for three time instants. The grey scale goes from 0 (the renovation process has not yet started) to 1 (100% renovation). The fluid flows from the left to the right.

[Figure 3 here]

[Figure 4 here]

From Figs. 3 and 4 it is observed that there is a full renovation of the fluid in almost half the volume of the digester at $t = 3.5$ h for the 666 m^3 h^{-1} flow rate, while this process is even faster for the high flow rate, showing a complete renovation in the whole volume at $t = 40$ min. The series of maps shows a gradual evolution of the tracer concentration along the digester, indicating that there are not any stagnation or by–pass region where the low velocities could worsen the mixing process and hence the digestion treatment.

As observed, the flow in the digester is mainly lead by the rotating motion of the four mixers, which enhances the mixing process between the original fluid and the tracer fluid. Each of them generates a kind of mixing cell where a more uniform distribution of the tracer's mass fraction can be seen. Also, it is noted that the flow between the cells is induced diagonally due to the alternate sense of rotation of the mixers (see Fig. 1), which is more clearly observed for the 4000 m^3 h^{-1} flow rate at $t = 10$ min. The diagonal flow is also evident in Fig. 5 (a), which presents the absolute velocity vectors near the two central mixers on a *xy* plane located at mid–height of the zone. In addition, the vector map of Fig. 5 (b), obtained on a mid–span *xz* plane, shows that the fluid flows near the axis of the mixers from the top side to the bottom of the digester. The fluid is

11

then impelled outside the mixer region while being lead to the top side again. This generates a structure in the flow at each mixing cell that resembles a toroid.

[Figure 5 here]

Equivalent contour maps for the aerobic digester are shown in Fig. 6 (666 m^3 h^{-1} flow rate) and Fig. 7 (4000 m^3 h^{-1} flow rate). In this case, the maps indicate that there is a very good mixture of the flow in the whole volume of the digester (the fluid flows from the right to the left), especially for the 666 m^3 h^{-1} flow rate, showing uniform final concentrations of the tracer with no presence of stagnation regions. At this low flow rate, it is seen in Fig. 6 that there is a full renovation of the fluid after about 4 hours of simulation. The renovation is even faster at 4000 m^3 h^{-1} flow rate (Fig. 7): about half the digester volume is full of tracer fluid after one hour of simulation. It is also noted that there is a better mixture of the flow at 666 m^3 h^{-1} flow rate than at 4000 m^3 h^{-1} flow rate: for a specific time instant, the differences between the higher and the lower concentrations observed in the contour maps are smaller for the former one.

[Figure 6 here]

[Figure 7 here]

The velocity vectors near the central region of the digester at 666 m^3 h^{-1} flow rate (mid–span vertical plane) are shown in Fig. 8. As observed, the flow is established from the bottom of the digester to its central region. This flow pattern induces a pair of vortexes, one at each side, which enhance the oxygenation of the fluid while improving the mixing process. This can explain the good uniformity in the tracer's concentration that was observed in the previous figures.

[Figure 8 here]

3.2. Estimation of time profiles and residence time distribution

The results obtained in the calculations were used to compute the Residence Time Distribution function, $E(t)$. This was done by storing the tracer's concentration, $C(t)$, at the outlet of the digesters during the transient tests. The concentration of the tracer at the inlet of the digesters was changed abruptly from 0 to C_0 like in a step experiment. In consequence, the normalized concentration of the tracer versus time profile at the exit boundary increases monotonically with time and it is known as $F(t)$ curve:

$$F(t) = \frac{C(t)}{C_0} \qquad (6)$$

The variable C_0 in the present work was set to $C_0 = 1$ (that is, a 100% of tracer fluid at the inlet). According to residence time theory [5], the relation between the function $E(t)$ and $F(t)$ in a step–like experiment can be expressed as:

$$E(t) = \frac{\mathrm{d}F(t)}{\mathrm{d}t} = \frac{\mathrm{d}C(t)}{\mathrm{d}t} \qquad (7)$$

13

that is, the function $F(t)$ or, equivalently, $C(t)$ in this case is the cumulative probability function of $E(t)$. For a specific time t_1, the cumulative probability function shows the fraction of the fluid that leaves the digester with an age below t_1.

The time profiles of functions $C(t)$ and $E(t)$ obtained in the anaerobic digester for the two test flow rates are presented in Fig. 9 (top) as an example of the procedure described. The grey curves correspond to the case $q = 4000$ m^3 h^{-1} and match the grey horizontal axis; the curve $E(t)$ for this flow rate is scaled by 1/7 to better fit the vertical axis. As expected, the $C(t)$ curves increase continuously with time for both flow rates until achieving a 100% concentration of the tracer at the exit of the digesters (mass fraction equal to 1), which takes place after about 7.5 h of operation for the low flow rate and after about 1 h for the high one. The profiles of $C(t)$ were used subsequently to compute the Residence Time Distributions $E(t)$ from Eq. (12), also shown in Fig. 9 (top). The $E(t)$ distributions are normalized so that the area below each of them is equal to 1.

[Figure 9 here]

In a wastewater treatment plant like the one investigated, a minimum residence time must be prescribed for the fluid in the digesters in order to assure a proper degree of water treatment. Thus, more relevant results are obtained in the analysis of 1-$C(t)$ curve rather than in that of $C(t)$ profile, since the former one shows the portion of fluid that leaves the digester with an age of, at least, a specific time t_1. In consequence, the curve 1-$C(t)$ for the two test flow rates is included also in Fig. 9 (bottom). The minimum, mean, and maximum residence times are defined for the percentile of 95%, 50%, and

14

5% respectively (95% and 5% instead of 100% and 0% in order to avoid the asymptotic effects of the curves). The magnitudes of these residence times (an example of the graphical determination for the low flow rate can be observed in Fig. 9, bottom) are summarized in Table 2 for both digesters; the time profiles obtained for the aerobic digester are qualitatively similar to those presented in Fig. 9 for the anaerobic one. In general, the smooth trend of all the profiles confirmed the good mixing of the flow and the lack of significant stagnation regions. The numerical predictions presented in Table 2 were contrasted with the experimental results available in the plant. The correspondence between the calculations of minimum, mean, and maximum residence times and the experiments resulted in a satisfactory agreement, showing maximum relative differences of about 5%.

[Table 2 here]

The numerical results were used also to estimate the renovation time in the digesters. This was done by computing along time the mass fraction of the tracer fluid in the whole volume of each digester. The renovation process can be considered as completed once the mass fraction is equal to 1 (100% of tracer fluid). In practice, a limit of 95% is established instead of 100% for the reason indicated above. The theoretical and the actual renovation times for the two test flow rates are presented in Table 3. The theoretical value was calculated simply as the quotient between the volume of the digester and the flow rate.

It is seen in Table 3 that the actual renovation time is in close relation to the maximum residence time (see Table 2) although the values are not strictly equal since the former is

related to the volume of the digester whereas the latter depends on the flow. The last column of Table 3 shows the ratio between the actual renovation time and the theoretical value. As observed, this ratio is below 2.3, which can be considered as low enough to indicate that there are not significant stagnation regions in the flow field. Also, it is noted that the performance of the anaerobic digester is slightly better due to the lower ratios and to the higher magnitude of the minimum residence time (see Table 2).

[Table 3 here]

The simulations were additionally used to investigate the mixing regime in the digesters, for which a mixing factor was defined. This parameter is the ratio between the volume–averaged velocity in the digester (calculated by CFD) and the theoretical averaged velocity (quotient between the flow rate and the cross–section of the digester). Although it is not any standard parameter, this mixing factor is used here to show a comparison between the actual mean paths of fluid particles in relation to the length of the digester (minimum distance required to flow from the inlet to the outlet). The results of these calculations are presented in Table 4.

It is seen in the table that, in general, the two digesters present a significant mixing: even in the most adverse conditions the fluid particles have to travel about 4 times the length of the digester. It is noted that the mixing induced by the diffusers in the aerobic digester is about one order of magnitude higher than that induced by the mixers in the anaerobic one. The volume–averaged velocity in the latter is quite independent of the flow rate since the flow is mainly lead by the rotation of the mixers. In contrast, it is

observed that the volume–averaged velocity within the aerobic digester is higher for the high flow rate. This is because the flow of air induced by the diffusers increases as flow rate is also increased. The results of Table 4 show that there is an inverse relationship between the mixing factor and the flow rate, which is more significant in the anaerobic digester due to the reasons indicated above.

[Table 4 here]

4. CONCLUSIONS

This article has presented a numerical investigation that was carried out in two open digesters of a full scale wastewater treatment plant. The methodology was based on the resolution of the 3D–URANS equations by means of a general purpose CFD code. Specifically, the commercial code Fluent® was used to estimate the residence time distribution in the aerobic and anaerobic digesters of the plant when operating at 666 m^3 h^{-1} and 4000 m^3 h^{-1} flow rate.

The approach used in the paper was to solve an additional transport equation for a tracer species with the same properties as the original fluid. This equation was resolved in order to get the concentration of the tracer along time, which was monitored at the outlet boundary of each digester to be related with the residence time of the fluid. This methodology provides a detailed description of the flow field that was used to detect stagnation and by–pass zones. Also, it allowed for the definition of a mixing factor that indicated the mixing regime in the digesters.

For the wastewater treatment plant investigated, the summary of the main conclusions deduced from the methodology is:

(1). The minimum residence times predicted were adequate for both digesters, showing better values for the anaerobic one.

(2). In general, a good mixing of the fluid was observed in all the digesters: the fluid particles have to travel at least 4 times the length of the digester in order to reach the exit boundary.

(3). The mixing is better in the aerobic digester than in the anaerobic one due to the upward forces induced by the grids of diffusers. The flow in the anaerobic digester is mainly lead by the mixers and hence the averaged velocities are quite independent of the flow rate.

(4). The fluid in the anaerobic digester flows downwards near the axis of the mixers, showing a flow structure that resembled a toroid.

(5). No significant stagnation or dead zones were observed in the flow fields.

ACKNOWLEDGMENTS

NOTATION

$C(t)$, C_0	species mass concentration function, reference concentration (p.u.)
$C_{\varepsilon 1}$, $C_{\varepsilon 2}$, $C_{\varepsilon 3}$	constants in the RNG k–ε model (-)
G_k, G_b	constants in the RNG k–ε model (kg m^{-1} s^{-3})
D_i	mass diffusivity (m^2 s^{-1})
$E(t)$	residence time distribution function (s^{-1})
$F(t)$	cumulative residence time distribution function (p.u.)
i, j	dummy index (-)
k	turbulent kinetic energy (m^2 s^{-2})
L	length (m)
m_i	mass fraction of species i (-)
$\bar{p}$	time–averaged static pressure (Pa)
q	flow rate (m^3 h^{-1})
R_ε	constant in the RNG k–ε model (kg m^{-1} s^{-4})
t	time (h)
u, v, w	velocity components in x, y, z direction (m s^{-1})

VC (t)	volume concentration function (p.u.)
W	width (m)
$\bar{v}$	time–averaged velocity (m s^{-1})
x, y, z	spatial coordinates (m)

Greek symbols

$\alpha_k, \alpha_\varepsilon$	constants in the RNG k–ε model (-)
ε	rate of dissipation (m^2 s^{-3})
μ_{eff}	effective viscosity (kg m^{-1} s^{-1})
ρ	density (kg m^{-3})

REFERENCES

[1] B. Newell, J. Bailey, A. Islam, L. Hopkins and P. Lant, Characterising bioreactor mixing with residence time distribution (RTD) tests, Water Sci. Tech., 37 (1998) 43–47.

[2] O. Levenspiel, Chemical Reaction Engineering, John Wiley & Sons, New York, 1999.

[3] D.A. Demidov, A.V. Krasnochub and A.V. Shepelin, Experimental Study of the Distribution Function of Water Residence Time in Disinfection Plants, Water Res., 28 (2001) 466–468.

[4] D. Olivet, J. Valls , M.A. Gordillo, A. Freixo and A. Sanchez A, Application of residence time distribution technique to the study of the hydrodynamic behavior of a full–scale wastewater treatment plant plug–flow bioreactor, J. Chem. Tech. Biotech., 80 (2005) 425–432.

[5] P.V. Danckwerts, Continuous flow systems. Distribution of residence times, Chem. Eng. Sci. 2 (1953) 1–13.

[6] A.D. Martin, Interpretation of residence time distribution data, Chem. Eng. Sci., 55 (2000) 5907–5917.

[7] F. Ghirelli and B. Leckner, Transport equation for the local residence time of a fluid, Chem. Eng. Sci. 59 (2004) 513–523.

[8] V.V. Ranade, An efficient computational model for simulating flow in stirred vessels: a case of Rushton turbine, Chem. Eng. Sci. 52 (1997) 4473–4484.

[9] G. Li, A. Mukhopadhyay, C–Y Cheng and Y. Dai, Various approaches to compute fluid residence time in mixing systems, Proc. of ASME 3rd Joint US–European Fluids Eng. Summer Meeting, 1–5 August, Montreal, Canada, 2010.

[10] B. Wu, CFD simulation of mixing for high-solids anaerobic digestion, Biotech. Bioeng. 109 (2012) 2116–2126.

[11] M. Terashima, R. Goel, K. Komatsu, H. Yasui, H. Takahashi, Y.Y. Li and T. Noike, CFD simulation of mixing in anaerobic digesters, Biores. Tech. 100 (2009) 2228–2233.

[12] H. Prieske, L. Böhm, A. Drews and M. Kraume, Optimised hydrodynamics for membrane bioreactors with immersed flat sheet membrane modules, Des. Water Treat., 18 (2010) 270–276.

[13] Y. Obikane, A computational method of a convective activated sludge model (ASM) in reaction tanks of wastewater treatment plants, Des. Water Treat., 33 (2011) 365–368.

[14] D. Diarra, S. Velaga, K. Lucka and H. Köhne, CFD analysis of mixing and residence time distribution in cool flame vaporizers. Proc. of the European Conference on Computational Fluid Dynamics, 5–8 September, Egmond aan Zee, The Netherlands, 2006.

[15] A.W. Patwardhan, Prediction of Residence Time Distribution of Stirred Reactors, Ind. Eng. Chem. Res., 40 (2001) 5686–5695.

[16] J.M. Bujalski, Z. Jaworski, W. Bujalski and A.W. Nienow, The Influence of the Addition Position of a Tracer on CFD Simulated Mixing Times in a Vessel Agitated by a Rushton Turbine, Chem. Eng. Res. Des. 80 (2002) 824–831.

[17] L. Zhang, Q. Pan and G.L. Rempel, Residence Time Distribution in a Multistage Agitated Contactor with Newtonian Fluids: CFD Prediction and Experimental Validation, Ind. Eng. Chem. Res., 46 (2007) 3538–3546.

[18] M.S. Vesvikar and M. Al-Dahhan, Flow pattern visualization in a mimic anaerobic digester using CFD, Biotech. Bioeng., 89 (2005) 719-732.

[19] B.E. Launder and D.B. Spalding, The Numerical Computation of Turbulent Flows, Comp. Meth. App. Mech. Eng., 3 (1974) 269-289.
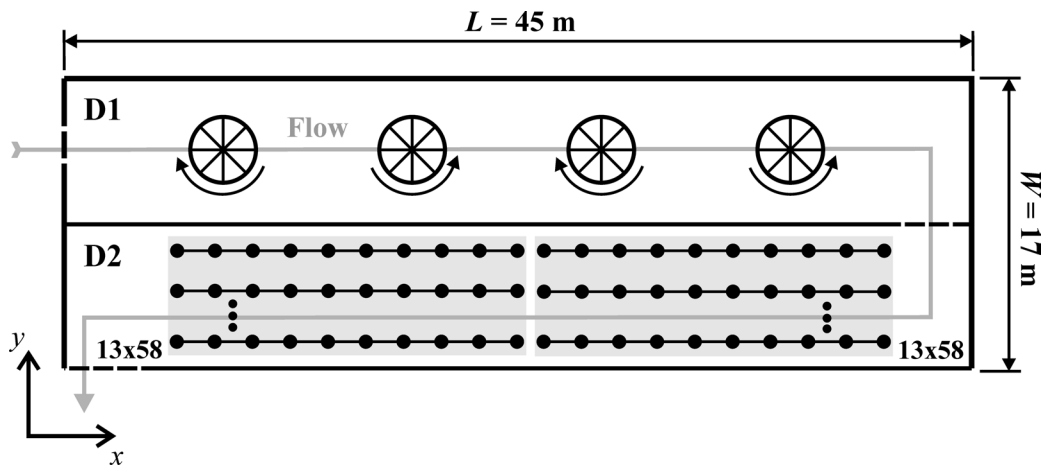
Figures

Figure 1. Basic arrangement of the digesters in the wastewater treatment plant
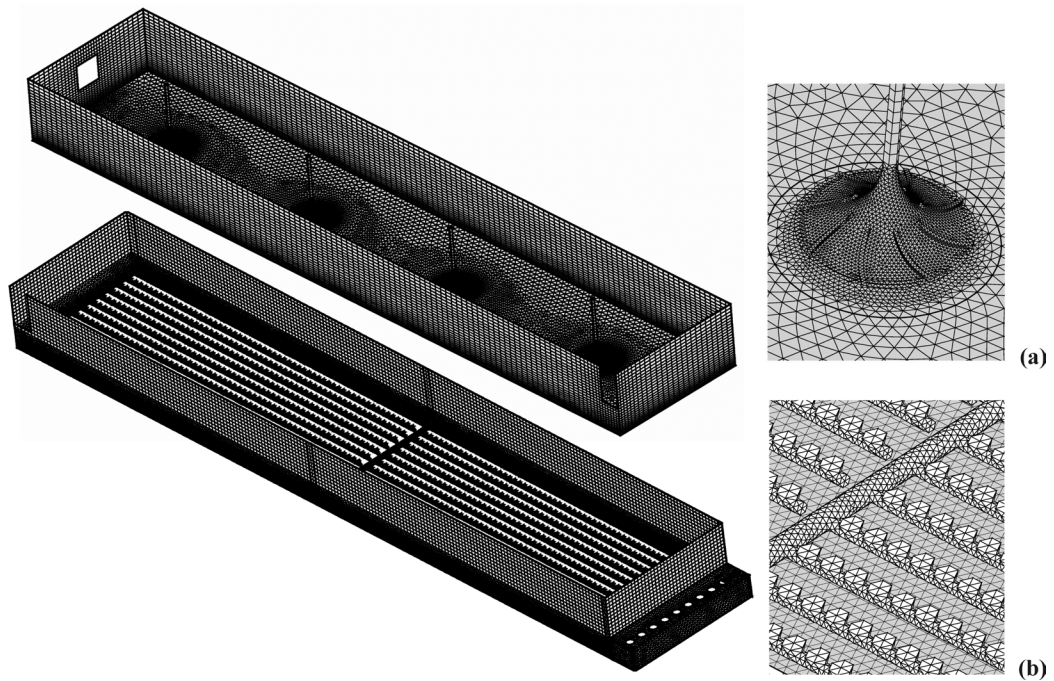
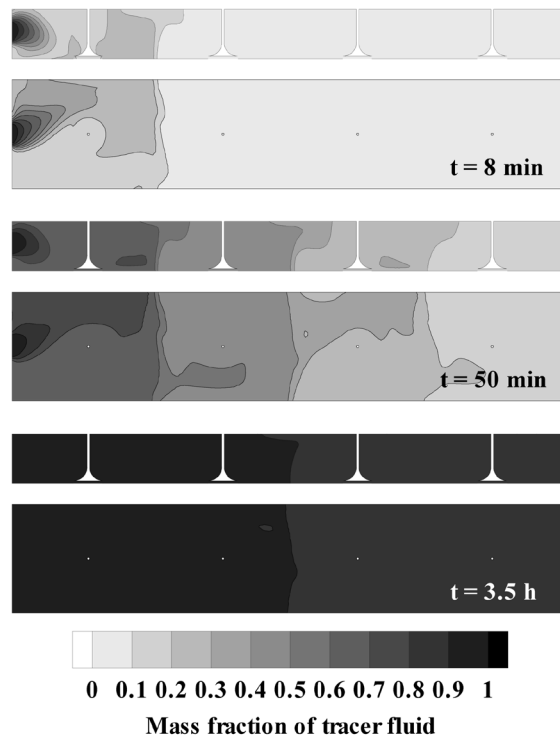**Figure 2.** Surface meshes of the digesters with a detail of the mixers and diffusers

Figure 3. Contour maps of the instantaneous mass fraction of the tracer fluid (D1) at
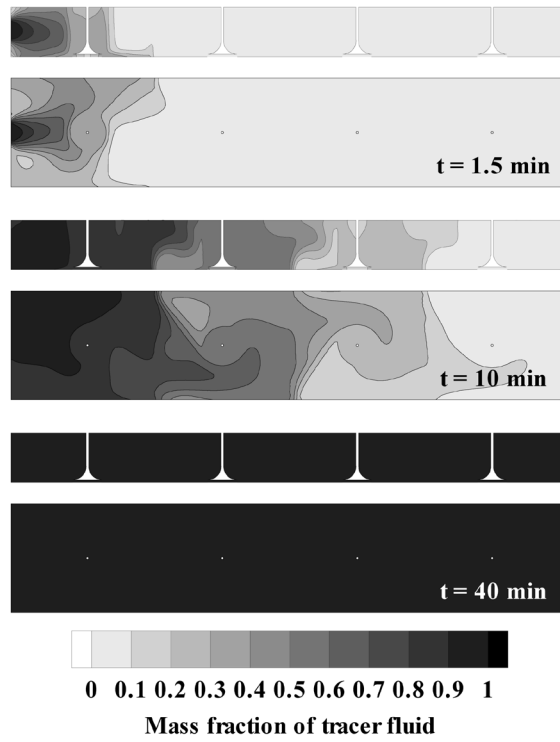
three time instants (666 m^3 h^{-1} flow rate)

t = 1.5 min

t = 10 min

t = 40 min

0   0.1 0.2 0.3 0.4 0.5 0.6 0.7 0.8 0.9   1

Mass fraction of tracer fluid

Figure 4. Contour maps of the instantaneous mass fraction of the tracer fluid (D1) at

three time instants (4000 m^3 h^{-1} flow rate)
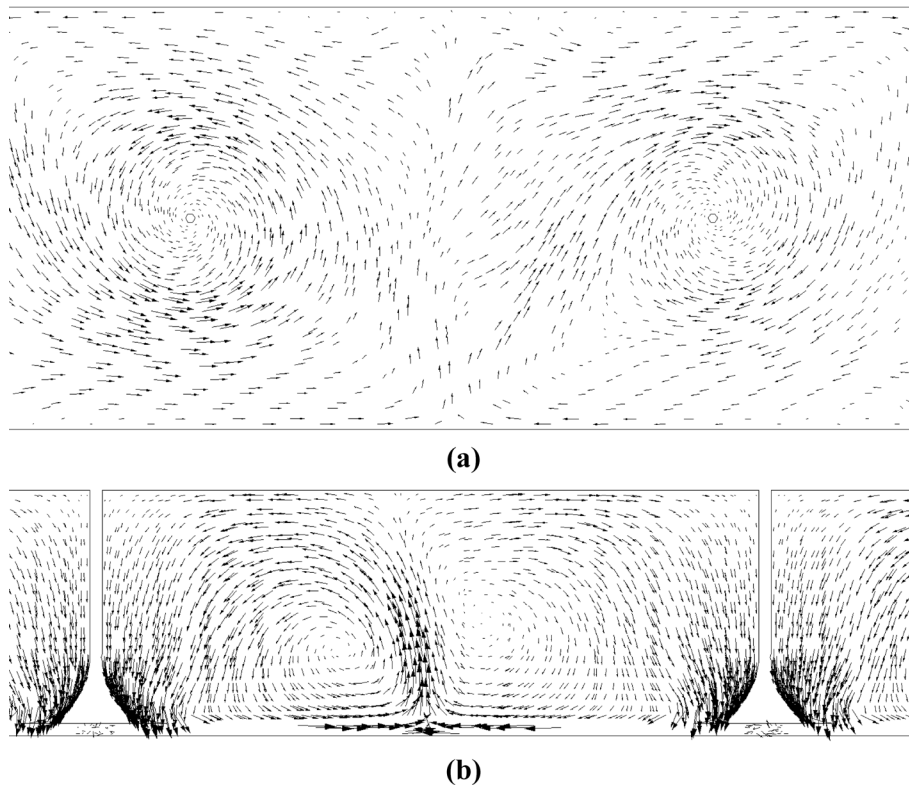
(a)

(b)

Figure 5. Velocity vectors near the two central mixers on a mid–height horizontal plane

(a) and also on a mid–span vertical plane (b). Results at 666 m^3 h^{-1} flow rate

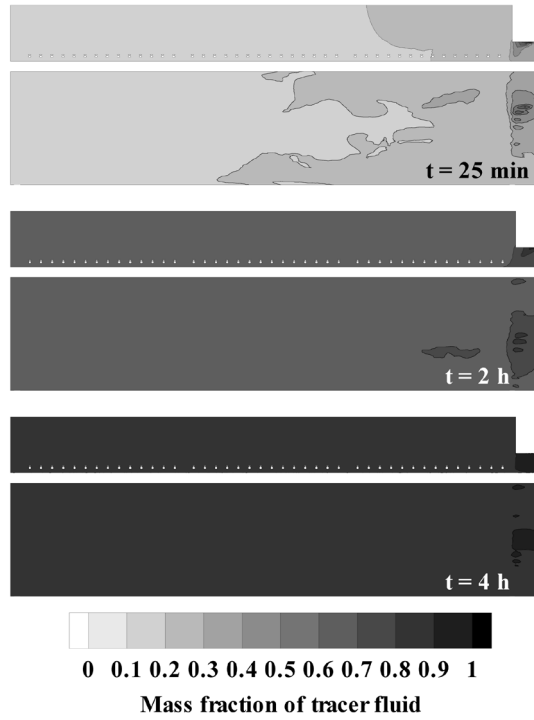**Figure 6.** Contour maps of the instantaneous mass fraction of the tracer fluid (D2) at
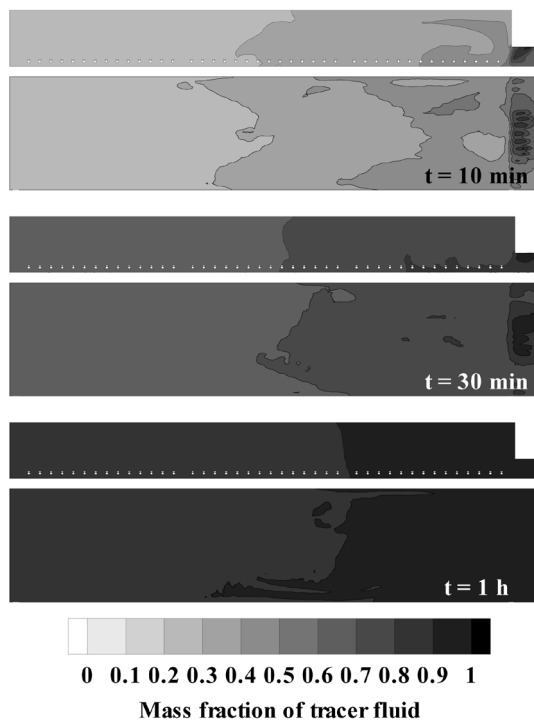
three time instants (666 m^3 h^{-1} flow rate)

Figure 7. Contour maps of the instantaneous mass fraction of the tracer fluid (D2) at
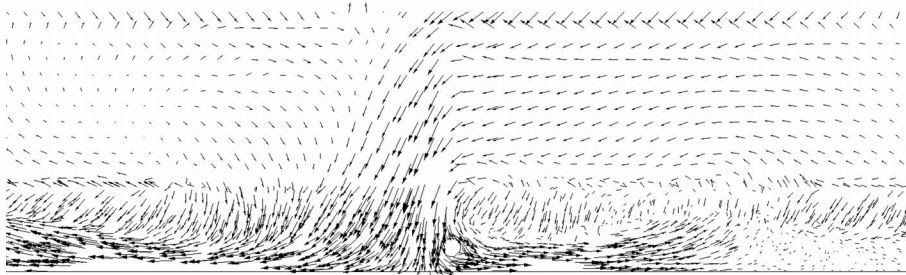
three time instants (4000 m^3 h^{-1} flow rate)

Figure 8. Velocity vectors (mid–span plane) near the central region of one grid of
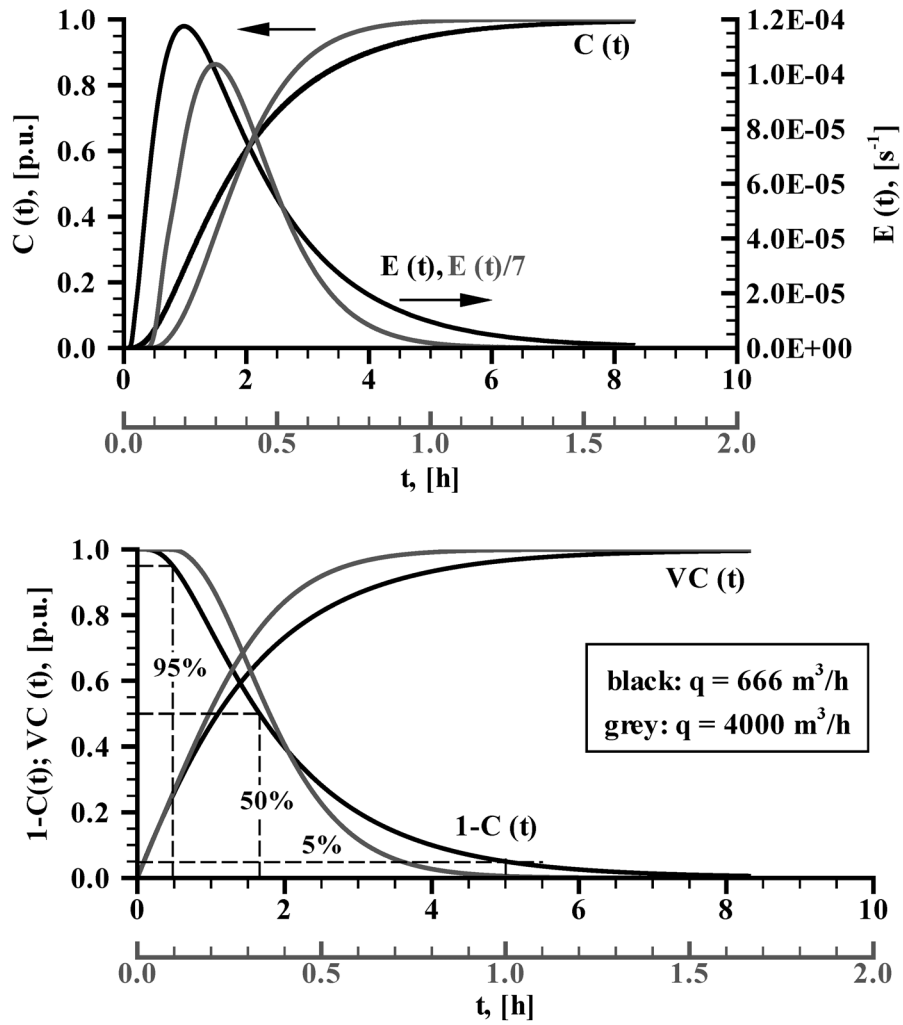
diffusers (666 m^3 h^{-1} flow rate)

Figure 9. Time profiles obtained in the simulations for the anaerobic digester and the

two test flow rates

Tables

Table 1. Grid size in each fluid zone

Digester	Number of cells
D1, anaerobic	401069
D2, aerobic	1229659
Total	**1630728**

Table 2. Minimum, mean, and maximum residence time

Residence time, t (h)			
$q = 666$ m^3 h^{-1}	TR$_{min}$ (95%)	TR$_{mean}$ (50%)	TR$_{max}$ (5%)
D1, anaerobic	0.48	1.66	5.00
D2, aerobic	0.29	1.35	5.11
$q = 4000$ m^3 h^{-1}			
D1, anaerobic	0.16	0.36	0.72
D2, aerobic	0.08	0.28	0.87

Table 3. Theoretical and actual renovation time

Renovation time, t (h)			
q = 666 m^3 h^{-1}	Theoretical	Actual (95%)	Ratio
D1, anaerobic	2.38	4.42	1.86
D2, aerobic	2.13	4.90	2.30
q = 4000 m^3 h^{-1}			
D1, anaerobic	0.40	0.57	1.43
D2, aerobic	0.35	0.79	2.26

Table 4. Mixing factors in the digesters

q = 666 m^3 h^{-1}	Theoretical average velocity (m s^{-1})	Volume-averaged velocity (m s^{-1})	Mixing factor
D1, anaerobic	0.0053	0.11	20
D2, aerobic	0.0059	0.39	66
q = 4000 m^3 h^{-1}			
D1, anaerobic	0.032	0.11	4
D2, aerobic	0.036	0.71	20